applied optics

Below the horizon—the physics of extreme visual ranges

Michael Vollmer

University of Applied Sciences Brandenburg, Department of Engineering, Magdeburgerstr. 50, 14770 Brandenburg, Germany
(vollmer@th-brandenburg.de)

Visual ranges of up to 440 km have recently been documented by photographs of ground-based observers. A report from 1948 claimed a record visual range from a plane of more than 530 km and a similar recent observation from 2017 was documented by a photo. Such extreme visual ranges can in principle be explained by the interplay of refraction and light scattering. However, they require optimal atmospheric conditions, and cleverly chosen locations and times.　　© 2020 Optical Society of America

1. INTRODUCTION

The greatest distance at which we can see an object through the atmosphere ranges from a few meters in thick fog to many kilometers in clear air. Even though only a few objects can be seen much further than 50 km away, sightings of extremely distant towering mountains have been documented by photographs.

In the past, theoretical maximum ranges (of around 330 km) have been discussed based on scattering in Rayleigh atmospheres (e.g., [1]). Respective early observations were rare (e.g., [2]). Nowadays, however, there are quite a few photo-documented extreme visual ranges well above 300 km. To our knowledge the present photo-documented world record visual range for a ground-based observer is 443 km [3]. In 1948, a record visual range observation was reported with a distance of more than 530 km from a plane in 4 km height near Cologne, Germany to the Mount Blanc in the Alps [4] and very recently a claim for a similar observation was made.

Theoretically, visual range is defined as the maximum distance a black object can be seen against the background sky. It depends on several factors including line of sight geometry, refraction, scattering and absorption of light in the atmosphere, and the sensitivity of the human eye. Requiring that very distant objects are detectable imposes constraints on the atmospheric constituents, on the height profile of the light path, on the lapse rates within the respective atmospheric layers, and on the irradiation of the air mass between object and observer. In this article we investigate the physics of extreme visual ranges, diagnosing each of the abovementioned factors in order.

2. GEOMETRICAL RECTILINEAR LINE VISUAL RANGE

For an observer at sea level with a height of the eye h_{obs}, the maximum line of sight distance of the horizon at sea level is [5]

$$x \approx \sqrt{2 R_E h_{obs}}. \tag{1}$$

More distant elevated objects of height h_{obj} extend this distance and the maximum line of sight distance is now the sum of the two distances (Fig. 1):

$$x \approx \sqrt{2 R_E h_{obs}} + \sqrt{2 R_E h_{obj}}. \tag{2}$$

Applying Eq. (2) to the symmetrical case where the Mount Blanc above the 4 km elevation level up to peak elevation 4.8 km was supposedly observed from a plane at elevation 4 km near Cologne, Germany, the line of sight is 451 km.

Because the actual distance between Mount Blanc and the location near Cologne is around 530 km, such a sighting is only possible because of refraction in the atmosphere.

3. VISUAL RANGE INCLUDING NORMAL REFRACTION

A. Normal Refraction in Regularly Layered Atmospheres

Rectilinear light paths work well for planets without atmosphere. Light on Earth, however, propagates almost always on curved trajectories due to refraction. French [5] quantitatively evaluated refracted light paths in a standard atmosphere. As a result, the observation distance for the horizon including refraction x_{refr} with regard to the rectilinear path x_{geom}, increases by up to 9% depending on observer height and the atmospheric
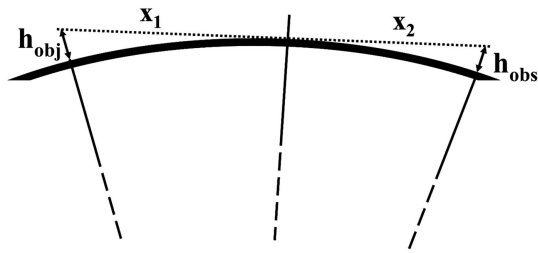
Fig. 1.   Geometry of finding the distance to an elevated object.

density profile. However, $x_{refr} = 1.09 \cdot 451$ km $= 492$ km still cannot explain a range of 530 km.

B. Anomalous Refraction

Temperature profiles of realistic atmospheres are characterized by lapse rates between $\alpha = 6.5$ K/km and $\alpha = 10$ K/km. Occasionally, abnormal situations with considerable changes of α exist due to inversion layers going along with sights of superior mirages [6–8]. As the index of refraction depends on pressure as well as temperature, light rays are bent differently in inversion layers which allows for much larger refracted ray distances.

A simplified discussion of how refraction depends on lapse rate was given by Young [9]. The model uses a horizontally stratified atmosphere, i.e., the surfaces of constant density are spheres. In this case, the light path is symmetrical with respect to the lowest point, nearest to the Earth surface. Young estimated the lapse rates α needed to produce rectilinear light propagation, the ones for light rays circling the Earth at constant height and he gave a crude estimate for the ray curvature $k = R_E / R$ for an arbitrary lapse rate α in K/km where R is the radius of curvature of such a ray:

$$k = \frac{35 - \alpha}{150}. \quad \textbf{(3)}$$

Figure 2 depicts a visualization of the main results of this model. For positive values of α the temperature drops with height (normal case) whereas negative values mean an increase of T with height as occurs in inversion layers. For $\alpha = +35$ K/km, the curvature is 0, i.e., $R \to \infty$, which resembles rectilinear propagation (the change of n due to the pressure drop with height is just compensated by the accompanying temperature drop). Larger lapse rates would lead to concave shapes. Rectilinear shapes are purely academic, concave shapes in nature sometimes happen close to heated ground, producing inferior mirages. The normal lapse rates in the atmosphere of between 6.5 K/km and 10 K/km (blue broken lines) correspond to radii of around 5.3 to 6 times the Earth radius. They explain the range extension discussed in Section 3.A.

The case $\alpha = 0$ occurs for a purely (hypothetical) isothermal atmosphere which gives $R \approx 4.3 R_E$ (green solid line). Inversions are characterized by $\alpha < 0$, which leads to smaller radii. For example, $\alpha = -115$ K/km results in a ray circling the Earth at constant elevation.

Figure 2 is just a simplified visualization. It holds if the whole atmospheric path of a light ray experiences the same lapse rate everywhere. In reality this is never true; however, one may expect ray curvatures along portions of the ray path with
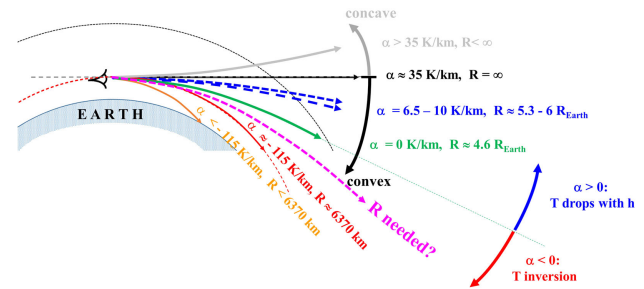

Fig. 2.   Schematic curvature of light rays in a concentric atmosphere with given lapse rates. An observer sees rays coming from the various directions indicated by the arrows.

appropriate lapse rate. The total path may then be constructed from all portions if the lapse rate along the whole path between observer and object is known. Unfortunately, complete data are usually not available. Therefore, the discussion of Fig. 2 shall only demonstrate that—depending on lapse rates in the atmosphere—different ray curvatures are possible, in particular smaller path radii than for normal conditions.

Figure 3 depicts potential conditions for the reported observation of around 530 km. From geometry alone [Eq. (2)] there is no allowed rectilinear light path between Mount Blanc and eye of the observer. Normal refraction can increase the range, but not enough to observe the mountain. If, however, the ray is bent stronger (lowest solid red line) in inversion layers, observation is in principle possible.

Justification for such ray paths comes from many reported superior mirage observations which require inversion layers in the atmosphere, sometimes with quite complex layer structure. Inversion layers are frequently occurring meteorological phenomena in the troposphere (e.g., [10]). In particular, the top of the planetary boundary layer (varying from around 500 m to up to 3 km above ground) is often combined with an inversion layer. Inversion layer data follow, e.g., from weather balloon ascents, radar or lidar measurements (e.g., [11,12]).

We briefly comment on one extraordinary mirage observation, the arctic Novaya Zemlya effect [13,14], which required abnormally bent light rays. The observation (at sea level) was that of an image of the Sun above the horizon, even though the Sun was geometrically 4.9° below the horizon. Lehn explained this phenomenon, where light rays of the Sun, after tangentially hitting the Earth surface, were trapped and traveled around 540 km around the Earth before reaching the eye of the observer! A prerequisite was an inversion layer which returned all rays traveling upward at angles below some specific value back toward the Earth. Most of the returning rays had Earth-grazing paths, which (due to curvature of the Earth) ultimately headed upwards, only to be returned again from the thermocline. This effect can develop properly only over flat featureless terrain,
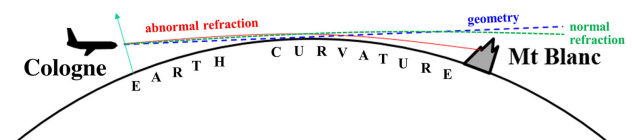

Fig. 3.   Schematic ray paths due to rectilinear geometry, normal refraction, and abnormal refraction due to inversion layers.

for which the temperature inversion exists over a sufficiently large area (such as the Arctic). Lehn estimated an inversion with maximum temperature gradient of 0.2°C/m to be sufficient.

This phenomenon proves that unusual refraction effects may indeed explain very long light ray paths in the atmosphere. Of course, requirements may be different for extreme visual range observations; however, we just assume that in principle, suitable conditions may exist and now discuss additional constraints due to processes in the atmosphere and the eye and brain.

4. PHYSIOLOGY AND PERCEPTION PSYCHOLOGY

The fact that the atmosphere allows light rays from an object to travel long distances and reach the eye of an observer is not necessarily sufficient for the perception of the object. The theory for calculation of horizontal visual range dates back to Koschmieder in 1924 [15] based on Fechner's law of perception. The latter states that any given perceived change (e.g., in brightness) is always related to the relative change of the stimulus (e.g., the incident radiation). An object will be recognized if it has a difference of either color or brightness with respect to its surroundings. Excellent summaries of the general topic of perception and visual range were given by Middleton [16,17]. He also extensively discussed the problem of color contrast for distant objects and concluded that in practice, colored objects at large visual ranges behave in the same way as gray ones. Therefore, we only focus on brightness contrast. As a consequence, an object is only visible when the ratio of the difference of luminance between the object and background and its background exceeds a certain value, the so-called contrast threshold C (e.g., [18–24]).

Following Koschmieder [15], a value of $C = 0.02$ is accepted as normal for the visual range of black objects during daylight. In Section 5 we will compute the distance associated with the contrast threshold.

Long-distance mirage observations usually show slightly fuzzy images due to spatial density fluctuations of the air and as a consequence of the index of refraction. The effects are sometimes called scintillation, twinkling, shimmer or—preferred by Middleton—optical haze [16]. Small-scale variations are caused by convection currents and usually happen after sunrise. For long visual ranges such index fluctuations will be promoted by turbulences, i.e., mixing of air masses along the line of sight. As fuzziness reduces contrast, observations for turbulent atmospheric conditions should be avoided. Here we assume optimum conditions, i.e., we neglect any scintillation effects.

5. VISUAL RANGE DUE TO ABSORPTION AND SCATTERING OF LIGHT IN THE ATMOSPHERE

The visual range due to absorption and scattering processes within the atmosphere has been widely discussed (e.g., [1,16,17,25–36]). The atmospheric constituents of the lower atmosphere are atoms, molecules, aerosols, water droplets, and ice crystals of various geometry. Obviously, each of these constituents may scatter and/or absorb electromagnetic radiation. The most simple case is given if only atomic and molecular gases are present (e.g., after heavy rain showers have washed out all aerosol particles). For such a clean atmosphere, scattering and absorption are lowest and the visual range will be largest.

Light passing through such an atmosphere is attenuated mostly via Rayleigh scattering. The radiance L_0 from an object which travels a distance x is attenuated due to scattering (and absorption) and is given by

$$L(x) = L_0 e^{-\beta(\lambda)x}, \tag{4}$$

where $\beta(\lambda) = \beta_{\text{Abs}}(\lambda) + \beta_{\text{Sca}}(\lambda)$ with $\beta_i(\lambda) = N_i \sigma_i(\lambda)$. Here, N_i are the number densities and σ_i are the respective cross sections which are tabulated or may be calculated [37,38]. For example, in the center of the VIS range around $\lambda = 560$ nm, $\beta \approx 0.0114/$km [37] at sea level (with $\beta_{\text{Abs}} \ll \beta_{\text{Sca}}$). A similar value of $0.0113/$km may be derived from the optical depth at sea level [38] and the scale height of 8 km of the atmosphere. Bohren [33] used $\beta \approx 0.0118/$km for $\lambda = 560$ nm at sea level.

Any illuminated distant object scatters light toward an observer, which is then attenuated due to Rayleigh scattering. In addition, the air molecules along the line of sight scatter Sun light, which is superimposed to the original scattered object light. For detection of the object, we require that the contrast exceeds the threshold value 0.02. The background may be another object, or it can be the adjacent sky. Various situations are possible (e.g., [16–18]) with brightly lit to black objects. In addition, the light path may be horizontal, or the observer could look up or downward at an angle. For simplicity, we only deal with horizontal paths. Furthermore, we assume black objects, which do not emit light themselves, and the horizon sky as background. In this case, the difference between object and background is just due to the difference of the perceived air light from object to observer with respect to the air light of the adjacent horizon sky.

The contrast calculation evaluates the air light by integrating the respective scattered radiance contributions from object or horizon to observer and therefrom calculates the corresponding luminances. As an approximate result, the contrast threshold C is finally related to the (wavelength-averaged) scattering coefficient β and the visual range d by [1,15,16]

$$-\ln(C) = \beta \cdot d. \tag{5}$$

For $C = 0.02$, $-\ln(C) = 3.912 \approx 3.9$ and one finds the famous Koschmieder formula

$$d = \frac{3.9}{\beta}. \tag{6}$$

For the sea level value $\beta = 0.0114$ km^{-1}, the visual range is about 340 km, in close agreement to the value of 330 km based on numerical evaluations [1].

Such large distances also explain why color contrast is not important for the threshold contrast criterion. Attenuated object radiation as well as air light close to the horizon (i.e., those radiances responsible here) is very close to being ideal white [39], i.e., a color contrast does not exist.

The above range estimate of 340 km is way below the needed 530 km. However, air density and light scattering from molecules decrease approximately exponentially with height h. As first typical approximation

$$\beta(h) = \beta_0 e^{-\frac{h}{H}}, \tag{7}$$

with the isothermal scale height $H \approx 8$ km. For example, at a height of $h = 3.56$ km, the scattering coefficient decreases to $0.641 \cdot \beta_0$ and the visual range correspondingly increases by a factor of $1/0.641$ to about 530 km. We conclude that a ray, circling around the Earth at an altitude of 3.56 km would allow visual ranges of up to 530 km. Although in principle possible, ray paths with such a radius of curvature are rather unlikely as they would require lapse rates of above 110 K/km in the atmosphere for extended distances (Section 3).

We also note that the theory can be easily extended to brightly sunlit objects (e.g., [27]) which may lead to even larger ranges.

6. ATMOSPHERIC CONDITIONS FOR OBSERVATION OF EXTREME VISUAL RANGES

Extreme visual ranges require first the existence of allowed light paths between the object and observer and second the necessary contrast above the threshold value (here 0.02) for detection with the eye. The discussion in Section 3 has demonstrated that in principle allowed light paths larger than 500 km may exist in the atmosphere provided the respective inversion layers with suitable lapse rates are present. In addition, the contrast condition may in principle be fulfilled if the effective atmospheric scattering coefficient β is sufficiently low, e.g., for light paths at high altitudes.

In the following, we combine these requirements and discuss atmospheric circumstances which may allow observation of extreme visual ranges. In particular, we discuss first effective scattering coefficients for oblique paths, second therefrom estimated atmospheric lapse rates for the respective light paths, and third the role of changes in the air light contributions due to inhomogeneous illumination of the path from object to observer, e.g., cloud shadows or before sunrise/after sunset conditions.

A. Effective Scattering Coefficients for Oblique Atmospheric Paths

Unless light rays circle the Earth at constant elevation, which is rather unlikely, one must always consider curved paths in the atmosphere which go along with a pressure variation. As a consequence, the amount of scattering depends on height. In order to compute the respective contrast and visual range, one must integrate along the ray path from the object and horizon sky to the observer. A simple rough approximation is depicted in Fig. 4. If the object and observer height are the same (as supposed for the Cologne/Mount Blanc example), the total light path is symmetrical, starting and ending at maximum height h_{max} and having minimum height h_{min} in the middle.

Switching from spherical geometry (a) to a flat Earth geometry (b), the curved light path from h_{max} to h_{min} may be very roughly approximated by a straight line. Assuming an exponential behavior of the scattering coefficient [Eq. (7)] we can calculate the attenuation of radiance along the straight line from h_{max} to h_{min} (and back again). Lambert–Beer–Bouguer's law [Eq. (4)] which enters all contrast and visual range calculations [Eqs. (5) and (6)] will still hold if we substitute β by an effective
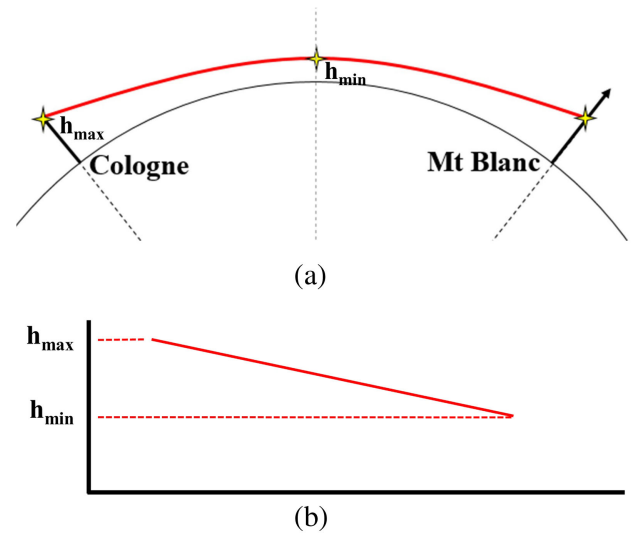

Fig. 4. (a) Geometry for curved light ray in spherical geometry and (b) most simple approximation of its left part in flat Earth geometry.

scattering coefficient β_{eff} given by

$$\beta_{eff} \approx \beta_0 \frac{H}{h_{max} - h_{min}} \left[e^{-\frac{h_{min}}{H}} - e^{-\frac{h_{max}}{H}} \right]. \tag{8}$$

Figure 5 depicts the variation of β_{eff} for given $h_{max} = 4$ km as function of h_{min} and the respective theoretical visual range according to Eq. (6). The effective scattering coefficient decreases with height [Fig. 5(a)], i.e., the larger the minimum height of the light ray, the less attenuation it suffers and the larger the respective visual range. The situation of $h_{min} = 4$ km corresponds to a spherical ray at elevation 4 km, whose scattering coefficient has decreased by a factor of $e^{-(4/8)} = 0.6065$ with respect to the sea level value. From the possible visual range (due to the contrast threshold) in Fig. 5(b), it is obvious that a range of 530 km requires a minimum height above 3 km.

This result will be used to construct possible light rays and judge the required lapse rates in the atmosphere necessary for these ray curvatures. The larger the minimum height, the smaller the radius of curvature of the light ray, and therefore the higher the necessary lapse rate. Therefore, we estimate the ray curvature and lapse rate for the limiting case of the minimum height of 3 km.

B. Required Lapse Rate for Given Minimum Height of Atmospheric Paths

Figure 6 shows the geometry [similar to Fig. 4(a)] of the Cologne/Mount Blanc example with a given minimum elevation (here $h_{min} = 3$ km) of the light ray if the object and observer are both at h_{max} (here 4 km). The coordinates of the observer in the plane above Cologne (P1) as well as the 4000 m level of Mount Blanc (P3) are known, as is the point of minimum height P2. We use $R_E = 6370$ km. The angle is given by the known distance between P1 and P3 of 530 km and amounts to 2.384°. If we assume for simplicity that all three points are part of a circular trajectory, the equation of a circle allows us to compute its center and radius, the latter being the radius of curvature of the light ray.
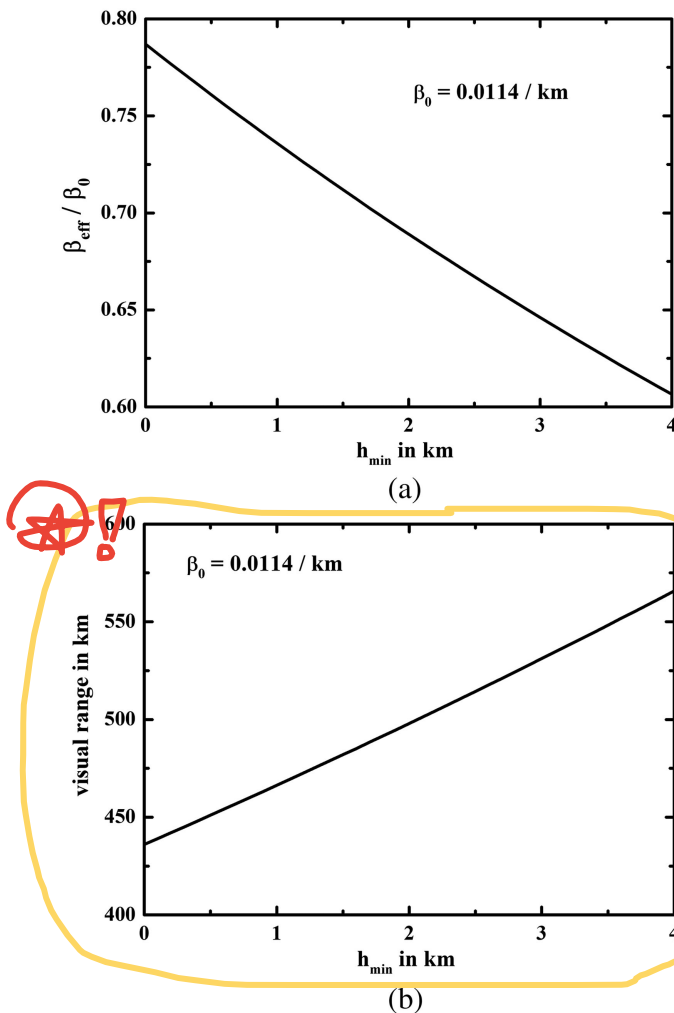
Fig. 5. (a) Decrease of effective scattering coefficient as a function of minimum height of the light ray (for $H = 8$ km, $h_{max} = 4$ km) and (b) corresponding visual range for a given wavelength averaged scattering coefficient β_0 at sea level.
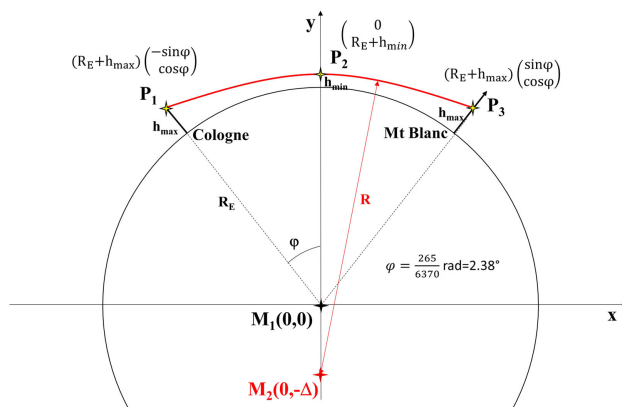

Fig. 6. Geometry for a symmetrical light ray with given minimum height.

We find a shift of the center with respect to the center of the Earth by $\Delta = 1412$ km, giving a radius of curvature of $R = 7785$ km.

From Eq. (3), $\alpha = 35 - 150 \frac{R_E}{R}$, the respective lapse rate is $\alpha \approx -88$ K/km, i.e., an inversion with roughly 0.9 K per 10 m elevation change. Obviously, such inversions are locally possible, however, it seems extremely unlikely that they occur over nearly the whole path length of more than 500 km. Therefore, we state again, that in principle the 530 km visual range is theoretically possible, however, extremely unlikely.

Of course it may be that other very rare conditions may exist which require less extended inversions and maybe wave-like ray paths with multiple oscillations between the object and observer; however, to be sure, one would need extensive meteorological data for the whole light path. This is usually not available with sufficient precision as it would require many locations with vertical temperature profile data of the atmosphere along the path to allow a respective simulation.

We believe that another factor, which happens much more often, may play an additional crucial role and may more realistically explain such long visual ranges.

C. Inhomogeneous Irradiation of the Light Path Between Object and Observer

Visual ranges were so far calculated from Eq. (6), based on the assumption that the complete path between the object and observer and beyond (for the horizon air light) was homogeneously irradiated. This holds well for clear skies during the day and is therefore the accepted standard, when discussing the meteorological visual range. However, there are also a few situations when this is not true. The most typical case is observing along a path which is partly in shadow due to higher lying clouds. The second frequently happening case is when observing distant mountains to the East in the early morning hours just before sunrise (or to the West after sunset). In this case, the silhouettes of the mountains are clearly seen against the already illuminated background sky whereas the path between the observer and the mountain may still be in complete or at least partial darkness. As a final example, inhomogeneous irradiation does also happen naturally during solar eclipses when part or the complete observed light path is within the umbra or penumbra. Indeed, it has been demonstrated and explained for distances of around 90 km, that such an inhomogeneous irradiation of the light path between the object and observer does increase the visual range [36]. The same effect—though using cloud shadows or before sunrise conditions—can also increase the extremely long visual ranges discussed here.

Let us assume the most simple situation, that only part of the light path (total length $d_1 + d_2$) with length d_2 close to the object is fully irradiated whereas the rest of length d_1 close to the observer is only partially irradiated with a fraction a of the full irradiation ($0 \leq a \leq 1$). This special case [36] led to the following modification of Eq. (5):

$$C = \frac{e^{-\beta d_2}}{\left(1 - a + \frac{a}{e^{-\beta d_1}}\right)}. \tag{9}$$

The special case $a = 0$, i.e., that part of the path close to the observer is in complete darkness, gives again Eq. (5) in the form $C = e^{-\beta d_2}$ where the total distance d is replaced by the smaller distance d_2. As $d_2 < d$, contrast increases and hence visual range

increases. As air light and object radiation are attenuated by the same amount in the dark region, contrast does not change any more.

With regard to extreme visual ranges, this means that if a large part of the atmosphere close to the observer is in darkness, the visual range can be drastically increased. This explains also why it is in principle possible to have very long visual ranges even if the atmosphere is not purely molecular. In practice, nearly every place on Earth is characterized by an atmosphere with some additional scattering due to haze. The total scattering coefficient would increase, reducing the visual range. If, however, part of the atmosphere close to the observer is in darkness, the range is extended, and even slightly hazy atmospheres may allow long-distance observations.

Imagine, e.g., a sea level light ray in a Rayleigh atmosphere with $\beta = 0.0114$/km as discussed above. It corresponds to a sea level maximum visual range of 340 km and a mountain range in this distance could be observed, provided there are allowed light path trajectories. If atmospheric haze particles would have an additional scattering contribution of the same magnitude, i.e., $\beta_{total} = 2\beta = 0.0228$/km, the visual range would be reduced by the same factor 2 to around 170 km. If, however, the second half of the path close to the observer is in shadow, it may still be possible to observe the mountain, which means the range would be extended.

We note that the situation is completely different if the dark region ($a = 0$) is close to the object. In this case, "object" and horizon sky radiance are the same and contrast is zero, i.e., the distant objects cannot be seen. Finally, sunrise observations (objects to the East) will provide better chances than sunset (objects to the West) as colder air after a cold night contains much less water vapor (a lot condensed on the ground) and thus the air will usually be less hazy.

7. DOCUMENTED RECORD VISUAL RANGES FOR EARTHBOUND OBSERVERS

The Internet is an extensive resource for fascinating photos of long visual ranges. Here, focus will be on a group of European naturalist photographers who have specialized in extreme long-distance photography [3]. Their website shows a collection of more than 50 selected long-distance photos with visual ranges above 100 km, most of them above 200 km, and around 10 above 300 km. Their experience let them investigate and chose those conditions, which are close to optimum with respect to the underlying physics as discussed above. For any visual range observation of more than 300 km, one needs the following ingredients:

(1) observer and object at high altitude;
(2) the light path must not be obscured by landscape topography;
(3) the atmosphere must be very clean (low humidity, no turbulences);
(4) inversion layers should allow for minimum light path heights of several kilometers;
(5) observations should preferably be before sunrise; and
(6) sufficient contrast between object and background.

Fig. 7.   Map including two observation sites in the Pyrenees and two observed objects in the Alps. Details, see text (image with some added distances and lines based on Google Maps).

The first two requirements define whether it is in principle possible to find a suitable object–observer pair. From Sections 2 and 3 it is best to have two mountain ranges, one with the objects and the other (with the need to be climbed) for the observer. In Europe, an obvious choice is the Pyrenees Mountains at the border between France and Spain and the (French) Alps (Fig. 7).

The Pyrenees mountain range has more than 200 peaks above 3000 m elevation (maximum 3404 m). The Alps have much higher mountains with 128 peaks above 4000 m (maximum 4810 m). In particular, the western Alps have very many high peaks above 3000 m. The distance between the Pyrenees and the Alps starts at around 350 km and extends well beyond 500 km. A look at topographical maps helps to avoid topographical obstacles (other nearer peaks) between selected individual peaks in the two ranges for observer and object. More simply, Google Earth generates height profiles for any given path between two points. In addition, the known Earth topography is very important for identification of the distant mountain peaks (see below).

The third and fourth requirements depend on meteorological conditions. It is well known for most locations on Earth that clear air conditions do exist, e.g., after extensive rain showers which have washed out any aerosols in the atmosphere. Inversion layers, on the other hand, also form frequently, e.g., at the atmospheric boundary layer. Therefore, such conditions may occasionally also exist for the chosen geometry between the Pyrenees and the Alps. Here, a weather report based personal experience of the photographers who know a certain region on Earth very well is extremely valuable.

The fifth requirement is important in connection with the discussion that an extension of the visual range happens only if the atmospheric part in darkness is close to the observer. As the Sun rises in the East, the observer must be in the West on a peak of the Pyrenees and the observed object will be a peak in the Alps. This was indeed the natural choice of the photographers.

The sixth and final requirement means that the eye (or the camera detector) must be able to first detect some signal at all and second detect differences of two adjacent object and background signals (contrast above threshold value). The best observation conditions are shortly before sunrise. The background sky to the west should already be bright enough. There is even one special optimum condition which can sometimes

be met, unfortunately only rarely. If the date and the pair of mountain peaks are properly chosen one can have the observer, the object peak, and the Sun at sunrise along one line, i.e., the background sky of the black object peak in the foreground is replaced by the much brighter reddish Sun at sunrise.

Bret and co-workers [3] have recorded many excellent photos demonstrating extreme visual ranges, in particular many of them from the Pyrenees mountains to the Alps. These examples also include some with the Sun just rising behind the silhouettes of distant peaks (e.g., the Tête de Chabrière in a distance of 381 km observed from Pic du Canigó [3]; see lower dotted red line in Fig. 7). These photos usually show a distorted shape of the Sun, nicely revealing the expected presence of inversion layers.

The photographers have summarized their personal experiences regarding atmospheric conditions and planning of trips for long-distance photography which are consistent with the presented physics [3]. The main problem of all extreme visual range photos is always the identification of the peaks. In advance they used horizon simulation programs, e.g., [40], which allow to show the panorama with topography in a given direction for chosen observation sites. Therefore, the longest visual range photos are usually not recorded by chance but planned in detail. The photographers know exactly what to look for.

The best conditions they have experienced have always been under very high-pressure conditions with calm, i.e., turbulent-free, air masses. Cloud covers or before-sunrise conditions were considered favorable. For any naked-eye observations, they recommend relative humidity to be below 30%, best conditions are for under 10%. Photographic evidence for distances below 300 km showed that not only black and white, but also color contrast could indeed be an issue. Common mountains (during the daytime) were usually detected as dark brown, but with increasing distance becoming light brown or even light blue due to the air light. Snow-covered peaks (in daylight) acting as white could sometimes get better contrast. For the very extreme long-distance observations discussed here, however, the photographers also recorded at sunrise when the mountains were not yet illuminated, thus acting as a black object versus the background sky.

The up-to-date record of a long-distance photo of an object is shown in Fig. 8. In this case, the Sun was not available as the background source, but rather the already illuminated morning sky was used. Figure 8(c) depicts the Pic Gaspard, a peak of 3867 m elevation in a distance of 443 km from the observer on Pic de Finestrelles at around 2820 m elevation before sunrise, July 16th, 2016 (middle blue dotted line in Fig. 7). A wider panorama is shown in Fig. 8(a) and the photo with some peaks identified in Fig. 8(b).

Figure 8(c) was recorded with a Panasonic Lumix FZ72 for ISO100, exposure time of 1/250 s, F2.8, and a zoom lens of 1200 mm. Again, the peaks were identified using the horizon simulation program [40]. The visual range must have been at least as large as 443 km as a peak in this distance could be observed.

The extraordinary conditions for such photographs are very rare. Bret meticulously planned the trip to record this photo for months in advance, carefully studying topographical maps and panorama simulations as well meteorological conditions in the region. Due to the latter it may well happen that one must
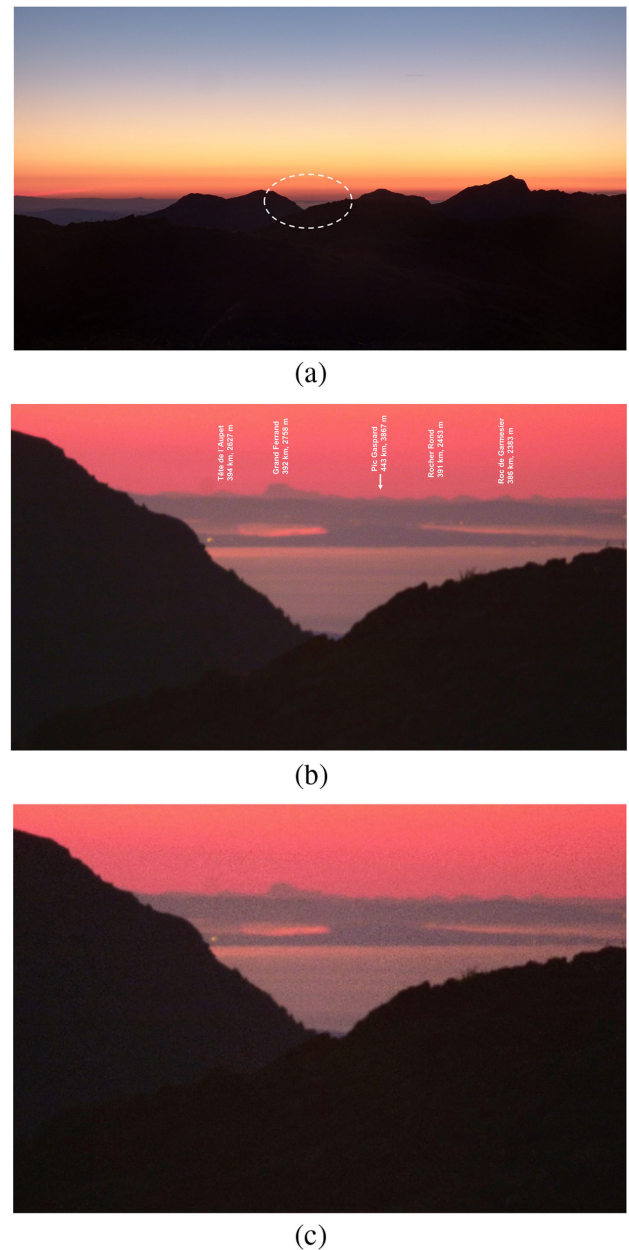

(a)

(b)

(c)

Fig. 8. Record long-distance observation of an Alps mountain peak in a distance of 443 km from the Pyrenees. (a) Scenery, (b) enlarged part with identified peaks, (c) original photo, courtesy photographer Marc Bret.

climb a mountain multiple times for a single good photo. Later he mentioned that probably the day of the photo was the best day of the whole year concerning visibility. Even for professional photographers, such extreme visual range observations are therefore more or less once in a lifetime observations.

8. RECORD VISUAL RANGES OBSERVED FROM AIRPLANES

According to Eq. (6), long visual ranges require small scattering coefficients, most simply realized by choosing high elevations of the observer. However, the maximum peak heights of mountain

ranges such as the Pyrenees are limited. Alternatively, one can use planes at higher elevation. One obvious advantage of such a scheme is that only one high mountain region (of the object) is needed. We first summarize our findings for the reported 530 km Cologne/Mount Blanc observation from 1948 before discussing another similar case.

Earth topography was not acting as an obstacle between Cologne and Mount Blanc. Just based on rectilinear geometry and normal refraction, such a visual range was not possible; however, abnormal atmospheric conditions, in particular inversion layers with given lapse rates, could have given rise to allowed light paths. As discussed above, an observer as well as object height of 4 km together with a light path of minimum height of 3 km would theoretically just allow the observation provided a pure mostly molecular atmosphere was present.

This seems rather unlikely; however, the observer could also have benefitted from inhomogeneous irradiation of the allowed light path close to the observer. Unfortunately, no time of day was given for the reported 530 km observation. Therefore, we can just guess that either during the day, part of the light path was in cloud shadows or—even more plausible—it was observed close to sunrise and a large part of the atmosphere was in darkness. In this case, even slightly hazy atmospheres would have allowed long ranges due to the respective range extension. To conclude: the reported visual range seems theoretically possible, however, only for quite special discussed circumstances; hence, some doubt remains.

Modern airplanes usually fly at higher altitudes. An observer elevation above 8 km already allows rectilinear light paths between a mountain peak of 4 km height (again the upper part of Mount Blanc) and the observer in a distance of around 545 km [Eq. (2)]. Normal refraction will increase this further, i.e., there is no need for special atmospheric conditions with inversion layers. The effective scattering coefficient of a respective purely molecular atmosphere would lead to a visual range of around 715 km [Eqs. (8) and (6)]. This means that additional scattering and absorption losses due to aerosols can still be tolerated for visual ranges of, e.g., 550 km. Therefore, extreme visual range observation conditions are easier to obtain than for Earthbound observers. However, airplane-based observations also have disadvantages.

First, there is the dependence on commercial time tables and flight routes—unless a chartered plane is used. Second, observations and recording of photos is often through scratched window panes with the additional problem of potential plane vibrations. Still, an impressive photo was recorded, again of Mount Blanc, from a distance of around 540 km (Fig. 9, [41]).

The photographer Ramon Ibarz was on a plane from Barcelona to Reykjavik passing Bordeaux at a cruising altitude of around 10,900 m. The location of the plane was estimated from the flight tracking app planefinder [42]. The photo was recorded August 22nd, 2017 at 06:36 am, about 17 min before sunrise using a Nikon D90 with 70 mm and 230 mm lenses. Identification of the peaks was realized using the panorama software [40] and the Mount Blanc peak is easily seen against the red morning sky. After identifying Mount Blanc and knowing the flight path of the plane, an observed distance of 538 km was calculated, which up to now seems to be the documented record
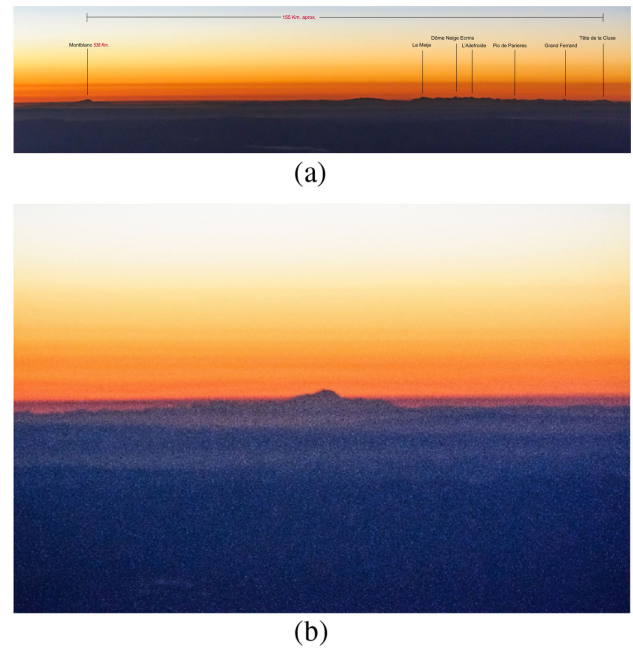

(a)

(b)

Fig. 9. Record airplane observation; (a) wider panorama; (b) Mount Blanc enlarged, from a distance of about 538 km (details, see text). Courtesy photographer Ramon Ibarz.

visual range observed from airplanes. The observation path is approximately indicated as the upper back line in Fig. 7.

9. OUTLOOK

Figure 8 effectively demonstrated that visual ranges of Earthbound observers of well above 400 km are possible. Figure 9 even extended this range above 500 km for observers on airplanes. An obvious question is whether there is a natural limit.

Classical observations for Earthbound observers are limited by the need of a suitable pair of mountain ranges and the fact that very special meteorological conditions are needed. In addition, there are constraints of minimum heights well above 3 km for low scattering coefficients if ranges above 500 km are chased, not to mention the problem in identifying individual peaks in a panorama with dozens of similar high mountain peaks. Therefore, the Pyrenees–Alps region may be at its limit already and the quest is open for any visionary mountaineer to study suitable places elsewhere on Earth [3].

In contrast, airplane-based observations allow conditions (height, direct path with normal refraction, low scattering) which are probably much easier to obtain and ranges of 600 km or beyond may be possible.

Disclosures. The author declares no conflicts of interest.

REFERENCES

1. C. F. Bohren and E. E. Clothiaux, *Fundamentals of Atmospheric Radiation* (Wiley, 2006).
2. W. E. K. Middleton, "Unusually great visual range over Ontario," Q. J. R. Meteorol. Soc. **61**, 411–416 (1935).
3. https://beyond-horizons.org/.
4. H. Berg, *Allgemeine Meteorologie – Einführung in die Physik der Atmosphäre*, (F. Dümmler Verlag, Bonn / Germany, 1948).
5. A. P. French, "How far is the horizon," Am. J. Phys. **50**, 795–799 (1982).
6. M. G. J. Minnaert, *Light and Color in the Outdoors* (Springer, 1993), older English ed., The Nature of Light and Colour in the Open Air (Dover, 1954).
7. R. Greenler, *Rainbows, Halos, and Glories* (Cambridge University, 1980).
8. D. K. Lynch and W. Livingston, *Color and Light in Nature*, 2nd ed. (Cambridge University, 2001).
9. A. T. Young, "Understanding astronomical refraction," Observatory **126**, 82–115 (2006).
10. M. Z. Jacobsen, *Atmospheric Pollution* (Cambridge University, 2002).
11. R. D. Garreaud, J. Rutllant, J. Quintana, J. Carrasco, and P. Minnis, "CIMAR-5: a snapshot of the lower troposphere over the subtropical Southeast Pacific," Bull. Am. Meteorol. Soc. **82**, 2193–2207 (2001).
12. B. B. Balsley, R. G. Frehlich, M. L. Jensen, Y. Meillier, and A. Muschinski, "Extreme gradients in the nocturnal boundary layer: structure, evolution, and potential causes," J. Atmos. Sci. **60**, 2496–2508 (2003).
13. W. H. Lehn, "The Novaya Zemlya effect: an arctic mirage," J. Opt. Soc. Am. **69**, 776–781 (1979).
14. W. H. Lehn and B. A. German, "Novaya Zemlya effect: analysis of an observation," Appl. Opt. **20**, 2043–2047 (1981).
15. H. Koschmieder, "Theorie der horizontalen Sichtweite," Beiträge zur Physik der freien Atmosphäre, Vol. **XII**, 33–53 (1924), "Theorie der horizontalen Sichtweite II," Beiträge zur Physik der freien Atmosphäre XII, 171–181 (1924); reprinted in Selected Papers on Scattering in the Atmosphere, C. F. Bohren, ed., SPIE milestone Series, Vol. MS7, SPIE, Bellingham (1989).
16. W. E. K. Middleton, *Vision Through the Atmosphere* (University of Toronto, 1952).
17. W. E. K. Middleton, "Vision through the atmosphere," in *Handbuch der Physik* (Springer, 1957), Vol. **48** (Geophysics II), pp. 254–287.
18. H. G. Houghton, "The transmission of light in the atmosphere with applications to aviation," J. Aeronaut. Sci. **9**, 103–107 (1942).
19. H. R. Blackwell, "Contrast thresholds of the human eye," J. Opt. Soc. Am. **36**, 624–643 (1946).
20. E. S. Lamar, S. Hecht, S. Shlaer, and C. D. Hendley, "Size, shape, and contrast in detection of targets by daylight vision; data and analytical description," J. Opt. Soc. Am. **37**, 531–545 (1947).
21. E. Pöppel and L. O. Harvey, "Light-difference threshold and subjective brightness in the periphery of the visual field," Psychol. Forsch. **36**, 145–161 (1973).
22. C. Owsley and M. E. Sloane, "Contrast sensitivity, acuity, and the perception of 'real-world' targets," Br. J. Ophthalmol. **71**, 791–796 (1987).
23. S. Verhulst and F. W. Maes, "Scotopic vision in colour-blinds," Vis. Res. **38**, 3387–3390 (1998).
24. K. Horváth, "Visibility in Geodesy," Periodica Polytechnica Civil Eng. **21**, 87–100 (1977).
25. H. G. Houghton, "On the relation between visibility and the constitution of clouds and fog," J. Aeronaut. Sci. **6**, 408–411 (1939).
26. R. G. Beuttell and A. W. Brewer, "Instruments for the measurement of the visual range," J. Sci. Instrum. **26**, 357–359 (1949).
27. G. Dietze, *Einführung in die Optik der Atmosphäre* (Akad. Verlagsges. Leipzig / Germany, 1957).
28. C. N. Davies, "Visual range and size of atmospheric particles," J. Aerosol Sci. **6**, 335–347 (1975).
29. C. A. Douglas and R. L. Booker, *Visual Range: Concepts, Instrumental Determination, and Aviation Applications* (National Bureaus of Standards Monograph, 1977), p. 159.
30. M. M. Meyer, J. E. Jiusto, and G. G. Lala, "Measurements of visual range and radiation-fog (haze) microphysics," J. Atmos. Sci. **37**, 622–629 (1980).
31. M. A. Ferman, G. T. Wolff, and N. A. Kelly, "The nature and sources of haze in the Shenandoah Valley/Blue Ridge Mountains area," J. Air Pollut. Control Association **31**, 1074–1082 (1981).
32. H. Özkayna, A. D. Schatz, G. D. Thurston, R. G. Isaacs, and R. B. Husar, "Relationships between aerosol extinction coefficients derived from airport visual range observations and alternative measures of airborne particle mass," J. Air Pollut. Control Association **35**, 1176–1185 (1985).
33. C. F. Bohren and A. B. Fraser, "At what altitude does the horizon cease to be visible?" Am. J. Phys. **54**, 222–227 (1986).
34. W. C. Malm, Introduction to Visibility, CIRA and NPS Visibility Program (Colorado State University, 1999), https://www.epa.gov/visibility/introduction-visibility.
35. S. Xiao, Q. Y. Wang, J. J. H. Cao, R.-J. Huang, W. D. Chen, Y. M. Han, H. M. Xu, S. X. Liu, Y. Q. Zhou, P. Wang, J. Q. Zhang, and C. L. Zhan, "Long-term trends in visibility and impacts of aerosol composition on visibility impairment in Baoji, China," Atmos. Res. **149**, 88–95 (2014).
36. M. Vollmer and J. A. Shaw, "Extended visual range during solar eclipses," Appl. Opt. **57**, 3250–3259 (2018).
37. R. Penndorf, "Tables of the refractive index for standard air and the Rayleigh scattering coefficient for the spectral region between 0.2 and 20 μ and their application to atmospheric optics," J. Opt. Soc. Am. **47**, 176–182 (1957).
38. B. A. Bodhaine, N. B. Wood, E. G. Dutton, and J. R. Slusser, "On Rayleigh optical depth calculations," J. Atmos. Oceanic Technol. **16**, 1854–1861 (1999).
39. D. K. Lynch and S. Mazuk, "On the colors of distant objects," Appl. Opt. **44**, 5737–5745 (2005).
40. U. Deuschle, Panorama creation program, https://www.udeuschle.de/panoramas/makepanoramas_en.htm.
41. https://beyond-horizons.org/2018/07/11/in-flight-pictures-mont-blanc/#more-2495.
42. Planefinder App, https://planefinder.net.